Identification of pancreatic stellate cell population with properties of progenitor cells: new role for stellate cells in pancreas

E Mato, M Lucas, J Pétriz, R Gomis, A Novials

Identification of pancreatic stellate cell population with properties of progenitor cells: new role for stellate cells in pancreas

E Mato*, M Lucas*, J Petriz, R Gomis, A Novials

* These two authors contributed equally to this study

See end of article for authors' affiliations

Correspondence to: Eugenia Mato, Networking Research Center on Bioengineering, Biomaterials and Nanomedicine (CIBER-BBN), Hospital Santa Creu i Sant Pau, Barcelona, Spain. Tel: 93 22919000, Fax: 93935565602, Email: emato@santpau.cat and Anna Novials, Diabetes and Obesity laboratory. Institute of Biomedical Research August Pi i Sunyer (IDIBAPS). CIBERDEM (CIBER de Diabetes y Enfermedades Metabólicas Asociadas), Hospital Clínic de Barcelona, C/Villarroel 170. 08036, Barcelona. Spain. Tel: 93 227 54 00 ext 4153, Fax: 93 4515272.; Email: anovials@clinic.ub.es

Abbreviations: SP, Side Population; ABC, ATP Binding Cassette; IAPP, Islet Amyloid Polypeptide; PaSC, Pancreatic Stellate Cells; MET, Mesenchymal-to- Epithelial Transition; HGF, Hepatocyte Growth Factor; BSA, Bovine Serum Albumin; MSC, Multipotent Fibroblast-like Cells; GFAP, Glial Fibrillary acidic protein

Running title
Pancreatic stellate cells have a progenitor role

SYNOPSIS

Numerous studies conducted in a diversity of adult tissues have reported that certain stem cells are characterized by the expression of a protein known as the ABCG2 transporter. In the adult pancreas, various multipotent progenitors have been proposed, however the ABCG2 marker has only been detected in the so-called Side Population.
In the present study we aim to identify new ABCG2+ pancreatic cell populations and to explore whether they exhibit properties of progenitor cells.
We isolated and expanded mitoxantrone-resistant cells from pancreata of lactating rats by drug selection. These cells were characterized and maintained in different stages of differentiation using several cocktail media plus matrigel. Differentiation was assessed by RT-PCR, immunocytochemistry, electron microscopy and ELISA methods.
The expanded cell population demonstrated a phenotype of pancreatic stellate cells (PaSC). Spontaneous cell clusters occurred during cell expansion and they showed weak expression of Pdx-1. Moreover, the presence of inductive factors in the Matrigel plus exendin-4 led to an increase in Pdx-1 and endocrine genes, such as insulin, IAPP, glucagon, GLUT2, chromogranin A, and convertases PC1/3, PC2 were also detected. Immunocytochemical analysis showed co-localization of insulin and c-peptide, while ultrastructural studies revealed the presence of granules. Insulin secretion of cell clusters was detected in the cell culture medium.
We have identified a population of PaSCs, which express the ABCG2+ transporter and have the capacity to transdifferentiate into insulin producing-cells. Although the potential therapeutic application remains to be tested, PaSCs could represent a future option in the research of insulin replacement in diabetes.

INTRODUCTION

The Multidrug Resistance Transporter ABCG2 has recently been identified as a molecular determinant of the Side-Population (SP) phenotype, a primitive hematopoietic cell population with a multipotential capacity. This transporter is also expressed in a wide variety of stem cells from adult tissue. It is considered as a novel stem cell marker, and it could be used, therefore, to localize and select these multipotent cells in different tissues [1-3].

In the case of the pancreas, there is no consensus on the nature or localization of adult stem cells [4,5]. Several authors have described transdifferentiation in different models in pancreas [6-10]. Also, experimental evidence indicates that the beta cell and other islet cells participate in the intra-islet regeneration [11-13]. Furthermore, a subpopulation of SP cells that co-express ABCG2, MDR1, and Nestin, have been identified and isolated from the adult human pancreas, and they may be a potential source of adult multipotential stem/progenitor cells useful for the production of islet tissue for transplantation into diabetic subjects [14]. However, it is not known whether, in addition to the SP phenotype, other types of pancreatic cells, such as the mesenchymal lineage, also express ABCG2 transporter and represents other adult stem cells that participate in endocrine differentiation.

In order to use adult pancreatic stem cells in potential therapeutic treatment for diabetes, we require more information on the lineage of these cells, the molecular mechanisms that allow them to remain undifferentiated, and the key factors that determine their differentiation [15].

Pancreatic stellate cells (PaSCs) are associated with diseases such as chronic pancreatitis and fibrosis [16,17]. Their hepatic counterparts have been described as exhibiting other properties, including those of progenitor cells, but in pancreas this role awaits further investigation [18]

The aim of this study was identify new ABCG2 (+) pancreatic cell populations and to explore whether they exhibit properties of progenitor cells.

METHODS

Selection of mitoxantrone-resistant cells and differentiation treatments

Fresh pancreata were removed from lactating rats, as approved by the Institutional Animal Care and Use Committee of the IDIBAPS Research Institute, Barcelona, Spain and digested with collagenase to obtain a primary cell culture. The cell digestion was rapidly divided in two homogenous suspension cells, one part was grown in Dulbecco's Modified Eagle Medium (DMEM) (Gibco-BRL, Gaithersburg, MD, USA) (25mM of glucose) supplemented with 10% fetal calf serum (FCS), 100 U/ml of penicillin (basal medium) was used as a control culture. The ABCG2 (+) cell line was generated by mitoxantrone (8μM) selection in the rest of the cell suspension. This drug acted through multidrug transporter systems and was diluted in the basal medium described before. The medium was removed every 2 days and it was gently washed to remove all the dead cells (Stage 1). The cells that survived of mitoxantrone exposition were then placed in fresh DMEM/F12 (11.1mM glucose) (Gibco-BRL, Gaithersburg, MD, USA) supplemented with 10% FCS. Mitoxantrone-resistant cells have the ability to proliferate until reaching confluence in a monolayer with a fibroblast-like appearance (Stage 2). In the stage 2, several 3D structures known as cell clusters appeared spontaneously, so-called (Stage 3). All the culture was maintained at 37ºC in a humidified atmosphere containing 5% $C0_2$. The cells were kept for about 2 years. Following drug selection, cell karyotype was analysed. The modal number of chromosomes (n = 42) was normal (data

not shown) and no loss of cellular phenotype was observed. Moreover, to confirm the presence of ABCG2 transporters, functional and expression studies were performed using flow cytometry, immunofluorescence and RT-PCR techniques (see methods below).

To induce cell differentiation, three media were tested for 3 weeks: **Medium 1;** DMEM (24mM glucose) supplemented with 10 ng/mL HGF (R&D Systems, Minneapolis), 0.5 pmol/L betacellulin (R&D Systems, Minneapolis) and 10 mM nicotinamide (Sigma); **Medium 2,** DMEM/F12 (11.1mM glucose) supplemented with 0.1 nM exendin-4 (Sigma); and **Medium 3,** DMEM/F12 (11.1mM glucose) supplemented with ITS (Insulin-transferrin-selenium) (Becton Dickinson) plus 0.1nM exendin-4 (Sigma). Matrigel was supplemented in Medium 3 as a base membrane preparation from Engelbreth-Holm-Swarm mouse tumour cells (Becton Dickinson). Matrigel was used following the manufacturer's instructions at a dilution of 1:3 and with one-hour gelling time at 37ºC. Inverted light microscopy was used to monitor morphological changes. In the differentiation experiments, 100 three-dimensional structures obtained from cell passages 12 to 15 were hand picked and dispersed using a solution of trypsin.

Measurement of apoptotic cell death

To assess drug selection, we analysed apoptosis of cells stained with Hoechst 33342 dye. The bis-benzimidazole dye penetrates the plasma membrane and stains DNA in cells without permeabilization. In contrast with normal cells, the nuclei of apoptotic cells have highly condensed chromatin that is uniformly stained by this dye. These morphological changes may be visualised by fluorescence microscopy. After exposure to mitoxantrone in growth medium, the cells on coverslips were fixed in 4% paraformaldehyde at room temperature for 20 minutes. They were then stained in the incubation buffer for 15 minutes with Hoechst 33342 dye at a concentration of 1 µg/ml. The morphological changes were examined under UV illumination using a fluorescence microscope (Olympus IX70-FL, Tokyo, Japan). The dye was excited at 340 nm, and emission was filtered with a 510nm barrier filter. To quantify the apoptotic process, cells with fragmented or condensed DNA and cells with normal DNA were counted. Data shows apoptotic cells as a percentage of total cells.

Flow cytometry

Flow cytometric analysis was performed with a FACScan flow cytometer (BD, San Jose, CA, USA) equipped with an argon-ion laser at 488 nm. Briefly, cells were harvested from the tissue culture flasks following treatment with trypsin. The cell suspension, at a concentration of 1.0 x 10^6 cells/mL, was fixed for 1 hour in 2% paraformaldehyde at 4ºC, washed once in PBS and stained overnight with primary antibodies, as summarized in Table 1. The labelled cells were analyzed on a FACS Calibur (Becton-Dickinson, Franklin Lakes, NJ, USA) by acquisition of 10,000 gated events. Data were stored as listmode files and analyzed with CellQuest (Becton-Dickinson, Franklin Lakes, NJ, USA) and Summit Workstation software.

Drug uptake and retention assays

To allow cell attachment to the surface and to obtain the conditions that would allow optimal growth. The cells were seeded in 12-well tissue culture plates (TPP, Trasadingen, Switzerland) at a final concentration of 1.0 x 10^5 cells/mL, 1mL total volume per well, 24 hours before the dye uptake/retention experiments. In the presence or absence of verapamil (5µM), drug uptake was measured by adding the fluorescent substrate (mitoxantrone 8µM) to the culture basal medium for 1 hour at 37°C. After 1

hour of incubation, cells were washed and resuspended in dye-free culture basal medium, and the blocker was maintained to evaluate its effect on dye retention. When dye compatibility was allowed, dead cells were excluded by simultaneous staining with 1 µg/mL propidium iodide (stock solution) [19].

Immunocytochemistry

Cells at distinct stages were plated in 8-well chamber slides (Nalge Nunc International, LAB-TEK). After fixation in 4% paraformaldehyde they were then blocked for 10 minutes at room temperature in 1% BSA and 0.2% saponin, and incubated overnight at 4°C with the primary antibody diluted in blocking solution (Table 1), following standard protocols. The bound antibody was visualised with a fluorescent secondary antibody (Table 1) under a Leica fluorescence microscope. 1% BSA was used instead of primary antibodies for control slides. In differentiation experiments, the total cells were isolated from cellular clusters and then spread on poly-L-lysine-coated slides, using a cytospin (Shandon Inc., Pittsburgh, PA, cytospin 3). The slides were subsequently fixed in ethanol/acetone (1:1vol/vol) for 10 minutes at -20 C and processed by immunocytochemistry techniques.

Oil red O-staining and vitamin A autofluorescence

The Oil red O-treatment for staining intracellular lipid droplets was performed in accordance with a modification of the method described by Lillie [20]. Briefly, cells were fixed with 4% buffered formalin for 10 minutes at room temperature, washed in PBS (twice, one minute each), and stained with a saturated solution of Oil red (Sigma, Taufkirchen, Germany) in acetone: ethanol (1:9) for 45 minutes at room temperature. Subsequently, cells were washed again under flowing cold water for 10 minutes, which resulted in red staining of lipid droplets. Finally, cells were examined by light microscopy.

Vitamin A storage in lipid vesicles was detected by fluorescence microscopy using an excitation wavelength of 320-380nm to visualize the characteristic rapidly fading fluorescent blue-green of this vitamin.

RT-PCR analysis

Total RNA was extracted from several stages of the cultures using RNeasy extraction kit (Quiagen). To remove genomic DNA contamination, DNase I (Invitrogen, Carlsbad, CA, USA) was used, following the manufacturer's protocol. One µg of total RNA was reverse transcribed in a buffer solution containing 25 nmol/L MgCl2, 100 mmol/L Tris (pH 8.3), 500 mmol/L KCl, RNAguard (39 U/mL; Pharmacia, Uppsala, Sweden), M-MLV-RT (200 U/mL; BRL, Gibco, Uxbridge, UK), 10 mmol/L deoxynucleotide triphosphate(s), and random hexamer priming [d(N6)5'PO4; Pharmacia]. Incubations of 30 minutes at 42ºC, 5 minutes at 94ºC, and 5 minutes at 5ºC were carried out in a total volume of 20 µL. Complementary DNA (cDNA) was stored at -80ºC until used. All PCRs were performed using 38 cycles. Parallel RT-PCR reactions without reverse transcriptase was performed for each sample. PCR products were visualized with 1 % agarose gel electrophoresis and ethidium bromide staining. The oligonucleotide sequences used for PCR amplification are summarized in Table 2.

Real Time-PCR

Real time PCR was performed using the double stranded DNA binding dye Power SYBR Green PCR Master Mix using the ABI Prism 7900HT Sequence Detection System (Applied Biosystems, Foster City, California, USA). The sequences of primers

used in this study are described in Table 2. A standard curve was generated from five serial dilutions of ARIP cell line synthesised cDNA for Pdx-1. Samples were analysed in triplicate, negative controls were included, and PCR products were verified using dissociation curve analysis immediately after RT-PCR. Expression of target gene was determined by normalising to the respective TATA Binding Protein (TBP) levels as a housekeeping gene. Results were analysed using SDS2.1 software (Applied Biosystems).

Infection of Recombinant Adenoviruse (Ngn3)

The adenovirus expressing mouse Neurogenin 3 (Ngn3) and a control adenovirus expressing bacterial β-galactosidase were prepared with the Adeno-X system (Clontech). For viral infection, cells were incubated with adenoviruses at a multiplicity of infection (MOI) of 50 for 2 hours at 37°C. The virus-containing medium was then replaced, and cells were cultured in the basal medium for 48 hours.

Assays for insulin secretion

Insulin secretion was measured by static incubation, as previously described [21]. Cells were plated in 12-well plates at 1.0 x 10^6 cells per well or 100 cell clusters (mitoxantrone-resistant cells at stage 3). Cells were pre-incubated for 1 hour in Krebs-Ringer buffer (KRB) and then incubated for 60 minutes at 37ºC in KRB containing 120mM NaCl, 5mM KCl, 2.5mM $CaCl_2$, 1.1mM $MgCl_2$, 25mM $NaHCO_3$, 0.1% bovine serum albumin and glucose at various concentrations. KRB media were collected and stored at -70ºC until they were assayed for insulin. Insulin was measured using an enzyme-linked immunosorbent assay (ELISA) kit (Mercodia, Uppsala, Sweden) that recognizes only mature insulin, following the manufacturer's instructions. This assay has <20% cross-reactivity with pro-insulin.

Electron microscopy

Cell clusters with and without Matrigel were pre-fixed in Karnovsky's fixative (2.5% glutaraldehyde and 2.0% paraformaldehyde) in 0.1 mol/L phosphate buffer (pH 7.3). The tissues were fixed in 1% freshly prepared osmium tetroxide and 0.8% potassium ferrocyanide in double distilled water for 1 hour. After 3 washes in cold double distilled water, the tissue blocks were dehydrated through an ascending concentration of acetone (30%, 50%, 70%, 95%, and 100%), and three changes of 100% acetone. They were then embedded in Spurr resin [22] and polymerized at 60°C. The embedded blocks were sectioned using a diamond knife (Diatome) on a Leica Ultracut UCT (Leica Microsystems, Deerfield, IL). Ultrathin sections were placed on a copper grid, and stained with uranyl acetate and lead citrate [23] before examination under a JEM 010 (Jeol Ltd., Tokio, Japan) equipped with a Gatan/MegaScan model 792 digital camera (Gatan Inc., Pleasanton, CA).

Statistics

Results are expressed as mean (SEM). The Student's *t* test was used for paired data. A p value of <0.05 was considered significant.

RESULTS

Establishment of ABCG2 (+) pancreatic rat cell culture

Several pancreata of lactating rats were collected and digested with collagenase. The specific drug mitoxantrone was then used for two weeks to select cells. A signal of

apoptosis was observed between days 2 and 4 after drug selection. This signal decreased significantly after the sixth day until its total negativization (day 12 of selection) (Fig1). After this period, several attached cells started to grow forming a monolayer phase with only one cellular phenotype identified as fibroblastoid-like cells (Stage 2) (Fig. 3B a,b). To determine whether mitoxantrone-resistant cells were able to increase drug accumulation, the intracellular drug concentrations of mitoxantrone were determined by flow cytometry in the unselected cells or after cell selection, described in the material and method, using verapamil as a specific ABCG2 inhibitor. As shown in Fig. 2 A, a significant increase of the intracellular concentration of the drug in the selected cells when the mitoxantrone plus verapamil was used. This increment was 129.8 %, but no significant increase was observed in the unselected cells, which was used as a control cell line. Moreover, gene expression of ABCG2 by RT-PCR confirmed that the primary culture of drug-resistant cells expressed this transporter (Fig. 2B).

Characterization of mitoxantrone-resistant cells

After cell drug selection, several cellular expansions without mitoxantrone were done. During cell growth, we can observe as three-dimensional structures (cell clusters) were formed in the cultures (Stage 3) with an average diameter of 29.8 µM±11.4 (Fig. 3B a,b,c,d,e). There was a 2.5-fold decrease in the proliferation ratio compared with that of the monolayer (data not shown), which indicated the presence of distinct cellular stages in the same cultures. Positive staining for Nestin and Thy1.1 (the two stem cell markers proposed) was observed in the cell obtained after cell selection and no evidence of positive signals were detected in the unselected cells (Fig. 3A). Moreover, although Cytokeratin 19 (CK19) was negative in all passages studied from mitoxantrone-resistant cells (supplementary Fig. S1 and Fig. S2 A), Nestin and Thy1.1 were positive. However, this positivity decreased in the highest passages from mitoxantrone-resistant cells, without negativization (supplementary S2 C). To confirm these results, gene expression analysis by RT-PCR was done with these markers in unselected cells (control cells) and in mitoxantrone-resistant cells. The results showed that while no signals were detected in unselected cells, the expression in the mitoxantrone-resistant cells was observed in both stage studies, (Fig.3C). However, when quantification of the progenitor markers (Nestin and Thy1.1) were assessed by flow cytometry, differences were detected between cells growing in mitoxantrone-resistant cells at stage 2 or in mitoxantrone-resistant cells at stage 3 (Nestin 85.97%±10.3 in Stage 2 vs. 29.5%±7.9 in stage 3; Thy1.1 91.3%±3.4 in Stage 2 vs. 12.9%±6.5 in Stage 3), without any significant differences in the mean fluorescence intensity (Fig.S2 C). Moreover, most of the mitoxantrone-resistant cells displayed strong labelling for N-CAM (Fig. 3 A) and also a strong auto-fluorescent signal was observed (Fig 3 A). To examine the phenotype of the mitoxantrone-resistant cell cultures, several markers were studied: vimentin (mesenchymal lineage), desmin (intermediate filament involved in the myogenic differentiation), alfa-actin (smooth muscle actin filament), GFAP (intermediate filament expressed in neural stem cells) and chromogranin A (present in secretory granules of neuroendocrine cells). All these markers were detected in mitoxantrone-resistant cells at stage 2 and stage 3 by immunocytochemistry (Fig. 4 A, B), and confirmed by RT-PCR (Fig. 4 C). However, the expression of these markers was slightly lower at stage 3 than in stage 2 confirmed by flow cytometry (supplementary Fig. S2 C). As cells showed a high auto-fluorescence signal, oil-red staining was performed to identify the presence of liposoluble material in the cell cytoplasm. Positive droplets were detected in the cytoplasm, thus confirming the presence of liposoluble material in the cell cytoplasm compatible with vitamin A in most of the mitoxantrone-resistant cells in our primary

culture. In addition, the percentage of oil-red staining observed in the slides was lower in the stage 2 than in the stage 3. Moreover, the characteristic fading fluorescent blue-green confirmed that these droplets corresponded to vitamin A. The overall characterization of our cultures indicated that the population selected corresponded to pancreatic stellate cells, the origin of which was mesenchymal. Moreover, the cells displayed several degrees of activation, as shown by the different amount of cytoplasmic vitamin A recorded between Stages 2 and 3 (Fig. 4 A, B).

***In vitro* endocrine differentiation of mitoxantrone-resistant cell (Stage3)**

Numerous studies suggest that the culture medium and the soluble factors added to the cultures play an important role in the maturation of different cell types [24]. The aim was to demonstrate the capacity of these selected cells to differentiate towards endocrine cells by means of media described in previous cell models (see material and methods). Medium 1 was used as a differentiation cocktail for three weeks. The mitoxantrone-resistant cells showed spontaneous differentiation when grown in basal medium DMEM/F12 (11.1mM glucose) with 10% FCS, as indicated by the presence of a weak band of Pdx-1 transcription factor. No difference in this gene was found when the cultures were treated with medium 1 (M 1) (Fig.5 A) [25]. Cultures obtained before cell selection (unselected cells) used as control cells and treated with the same medium (M1) were always negative (Fig. 5 A). However, a weak signal corresponding to the transcript of the neurogenin 3 gene (*Ngn3*) was observed only in treated mitoxantrone-resistant cells with M1 (Fig. 5 A). This gene plays a key role in beta-cell differentiation [26]. To verify whether other genes implicated in the endocrine differentiation pathway could be induced *in vitro*, isolated cell clusters from mitoxantrone-resistant cells at stage 3 were infected with an adenovirus neurogenin 3 construct. After infection, there was an increase in Pdx-1, as well as in other transcription factors that were detected earlier, such as Neuro D and Pax-4, both of which are involved in endocrine cell differentiation (Fig.5B). Quantitative Real-Time RT-PCR indicated that both media (M1 and M2) increased 3.9-fold±2.9 and 4.9-fold±3.4 respectively Pdx-1 mRNA basal expression ($n=3$, $p<0.05$, Fig.5C). Moreover, the medium 2 (M2) that was supplemented with exendin-4 indicated a higher increase compared with the medium 1 (M1). Exendin- 4 is known to produce activity in islet cells in the pancreas via GLP-1 receptors, giving rise to beta-cell activity and insulin release. It also participates in control of glucose and in fat metabolism. In addition, the presence of GLP-1 receptors confirmed by RT-PCR indicates possible effects in these cells (Fig. 5C). Finally, in order to simulate a specific cellular niche for endocrine differentiation, 100 cell clusters were cultured with matrigel as a semisolid medium supplemented with exendin-4 (M 3). After two weeks of culture under these experimental conditions, the transcription of Pdx-1 increased. In addition, a strong insulin signal was detected for the first time. Moreover, IAPP, glucagon, GLUT2 and the convertases PC1/3 and PC2 were also detected after this treatment (Fig 5A). In contrast, expression of the transcription factor p48 and other exocrine genes, such as amylase, were not detected (data not shown). Interestingly, CK 19 expression was observed. Flow cytometry showed that 31.21%±5.2 of cells were c-peptide positive, and 39.54%±2.1 were also positive for Pdx-1, while a few cells were positive for Nestin 0.8%±0.065. In addition, insulin and c-peptide were co-localized in all the cells studied (Fig. 6). We also observed that c-peptide co-localized with vimentin and CK19 in some cells, but not with the other markers studied (alpha-actin and GFPA) (Fig.6). Moreover, ultrastructural studies showed that the monolayer cells displayed characteristics compatible with activated pancreatic stellate cells: extensive hypertrophy of the rough endoplasmatic reticulum (RER), abundant lysosomes in the cytoplasm, few lipid

droplets and the presence of abundant fibers of collagen in the extracellular compartment (Fig. 7A a-d). The clusters that grew in Matrigel plus exendin-4 showed substantial ultrastructural changes, with smaller and homogenous cell size, with round nuclei and electron-dense homogenous chromatin, a significant increase in the number of mitochondria, lipid droplets in their cytoplasm and also abundant electron-dense granules were also observed (Fig. 7A e-h).

Finally, insulin secretions of several sets of cell clusters were measured by static incubation at low (2.8mM) and high (20mM) levels of glucose. Insulin secretory response to high glucose increased by 44% (911.8 ± 31.7pg /cell cluster) vs. low glucose (635.7±13.4pg /cell cluster) ($p<0.05$) (Fig. 5B). However, insulin secretion in undifferentiated cells obtained during the first expansion phase of the mitoxantrone-resistant cell (Stage 2), was below the detection limit for the two glucose treatments tested (Fig. 7B).

DISCUSSION

The therapies currently used to treat diabetes are unsatisfactory, as they do not offer a cure and cannot prevent the development of the complications associated with the disease [27]. The need for new therapeutic strategies, including genetic and cellular approaches, has led researchers to explore alternative cellular sources of insulin-producing cells, such as embryonic stem cells or stem cells isolated from adult tissue [28]. There is considerable controversy regarding the progenitor of the pancreatic endocrine beta-cell tissue. Ductal, acinar, SP and, very recently, multipotent fibroblast-like cells (MSCs) in the adult human exocrine pancreas have all been proposed as potential progenitors [29,30]. However, the specific signals that induce transdifferentiation, as well as the proliferative signals to expand a specific type of progenitor, must be identified [31-33]. Moreover, to identify multipotential cells, specific cell markers are required. The mechanisms controlling islet cell neogenesis are largely unknown. The formation of new islets, as seen from the ductal epithelium, has long been considered one of the mechanisms of normal islet growth after birth and in regeneration and suggests the presence of pancreatic stem cells. It has been documented that there are abundant endocrine progenitor cells in the neonatal pancreas, but little is known about their relative proportions or even phenotypes. Two candidate precursor markers have been proposed: a haematopoietic stem cell marker, c-Kit, and a neural stem cell marker nestin. In a pre- and post-natal rat pancreas, these two markers decreased proportionally with age, coinciding with the appearance and development of endocrine cell types [34]. Multidrug transporter systems, and more specifically, the ABCG2 subtype, have been proposed as a new marker of stem cells. In the human pancreas, this marker has been identified in the primitive hematopoietic stem cells with SP phenotype, located in the islet or around acinar cells. Other pancreatic cells that can express this marker, however, have not yet been investigated [35]. Rats and mice express the ABCG2 gene in several tissues, such as intestine, kidney and testis, but the pancreas has not been investigated to date [36].

Although the precise physiological function of these transporters in progenitor and differentiated cells is unknown, it has been postulated that they confer protection against a number of xenobiotics, thus maintaining the regenerative capacity of the tissue [37].

Here we isolated ABCG2 (+) cells with mesenchymal features from adult pancreatic tissue of lactantig rats. Because of their capacity to adhere and to divide quickly, these cells were maintained in culture, as a cell line, for more than two years. This approach allowed us to characterize these cells. We demonstrate that ABCG2 (+) cells correspond to a population of pancreatic cells known as pancreatic stellate cells. Although their

origin is still being debated, they share the characteristics of mesenchymal (vimentin), neural (GFAP) and muscular (desmin and alfa- actin) cells. One of the main characteristics of stellate cells is their capacity to transdifferentiate. When activated, they express alfa-actin and produce many collagen fibers. They thus resemble myofibroblast cells and may, therefore, be involved in tissue repair [38,39]. Recently it has been described that CD133+ hepatic stellate cells exhibit the properties of progenitor cells and display the capacity to develop into endothelial-like and hepatocyte-like cells *in vitro* [18]. Our study demonstrates that, although stellate cells are not currently considered true stem cells, they share specific markers with other known adult stem cells, such as ABCG2, Nestin, Thy1.1, and N-CAM. The latter participates in signal transduction and in cell type segregation as a mediator of cellular junctions during organogenesis [40].

Although PaSCs do not usually express endocrine genes during cell expansion, spontaneous cell differentiation occurred and these cells showed weak expression of Pdx-1 (a key transcription factor in the endocrine differentiation pathway). Few studies are investigated regarding how culture medium and additional protein components affect the viability and maturation of the cell [41]. Our results underscore the importance of defining culture medium composition in experimental procedures in order to identify new soluble factors involved in the processes of cellular transdifferentiation. Moreover, to identify instructive signals that induce differentiation during organogenesis, it will be important to determine how such signalling networks are established and how they elicit multiple signalling responses in endodermal cells to activate appropriate genetic programs [42]. Several signalling molecules have been implicated in induction of specific endodermal cell types. However, few of these factors have been examined in adult pancreatic tissue [43]. Here it is shown that the presence of inductive factors in the extracellular matrix, in addition to other substances participating in pancreatic differentiation, such as exendin-4 (GLP-1 analog), are required to proceed to the transdifferentiation stages in our cellular model. GLP-1 is secreted from the L-cells of the distal ileum and colon; however, numerous studies show that GLP-1 produces an increase in the beta-cell mass by inducing the neogenesis and transdifferentiation of ductal progenitors into islets cells through the expression of Pdx-1 [44-46]. Soluble factors secreted by PaSC are important in pancreas physiology including matrix turnover processes. However, other roles including effects on progenitors have not been investigated. The analysis of PaSC secretome conducted by our group has identified three new proteins: PEDF, LIF and Wnt5b involved in differentiation and developmental processes described in different cellular models [data not shown]. Future experiments will be required to demonstrate that these proteins are able to participate in the spontaneous Pdx-1 expression detected in the culture from mitoxantrone-resistant cells and may also contribute to the high CK 19 expression detected after cell differentiation.

In summary we found that mitoxantrone-resistant cells obtained from lactating rats pacreata, express the ABCG2 transporter, has a PaSC phenotype and they are able to secrete insulin after cell differentiation.

ACKNOWLEDGEMENTS

The authors thank Scientific and Technical Services of the University of Barcelona (SCT-UB, Campus Casanova) for technical support with electron microscopy, Rosa Gasa for the AdCMV-ngn3 and AdCMV-β-gal constructs, Margarita Nadal for the kariotype assistance and Caroline Newey for editorial assistance.

This project was funded by grants from PI020881, RCMN C03/08, PI042553, SAF 2003-06018, SAF 2006-07382 and RGDM G03/212 and by Sardà Farriol Research Program. The CIBERDEM and CIBER-BBN are an ISCIII project.

Authors' affiliations
E Mato[1, ¶], M Lucas[1], J Petriz[3, #], R Gomis[1,2], A Novials[1,2]

1 Diabetes and Obesity Laboratory. Institute of Biomedical Research August Pi i Sunyer (IDIBAPS), Barcelona
2 CIBERDEM (CIBER de Diabetes y Enfermedades Metabólicas Asociadas), Hospital Clínic de Barcelona. Spain
3 Cryopreservation Unit, Clinic Hospital/IDIBAPS, University of Barcelona. Barcelona, Spain.
¶ Networking Research Center on Bioengineering, Biomaterials and Nanomedicine (CIBER-BBN), Hospital de la Santa Creu i Sant Pau, Barcelona, Spain

Current address: Jordi Petriz, Laboratori 123, Institut de Recerca, Hospital Universitari Vall d'Hebron, P Vall d'Hebron 119-129, 08035 Barcelona, Spain.

Conflict of interest: None declared

REFERENCES

1 Zhou, S., Schuetz, J.D., Bunting, K.D., Colapietro, A.M., Sampath, J., Morris, J.J., Lagutina, I., Grosveld, G.C., Osawa, M., Nakauchi, H., Sorrentino, B.P. (2001) The ABC transporter Bcrp1/ABCG2 is expressed in a wide variety of stem cells and is a molecular determinant of the side-population phenotype. Nat. Med. **7**,1028-1034

2 Bunting, K.D. (2002) ABC Transporters as Phenotypic Markers and Functional Regulators of Stem Cells. Stem Cells **20**,11-20

3 Krishnamurthy, P., Schuetz, J.D. (2005) ABCG2/BCRP in Biology and Medicine. Annu. Rev. Pharmacol. Toxicol. 381-410

4 Bonner-Weir, S., Sharma, A. (2002) Pancreatic stem cells. J. Pathol.**197**, 519-526

5 Bonner-Weir, S., Toschi, E., Inada, A., Yatoh, S., Li, W.C., Aye, T., Toschi, E., Sharma, A. (2004) The pancreatic ductal epithelium serves as a potential pool of progenitor cells. Pediatr. Diabetes **5** Suppl **2**, 16-22

6 Von, Herrath, M., Homann, D. (2004) Islet regeneration needed for overcoming autoimmune destruction - considerations on the pathogenesis of type 1 diabetes. Pediatr. Diabetes Suppl **2**,23-28

7 Gao, R., Ustinov, J., Korsgren, O., Otonkoski, T. (2005) In vitro neogenesis of human islets reflects the plasticity of differentiated human pancreatic cells. Diabetologia **48**,2296-2304

8 Rosenberg, L. (1998) Induction of islet cell neogenesis in the adult pancreas: the partial duct obstruction model. Microsc. Res. Tech. **43**,337-346

9 Rosenberg L, Duguid WP, Healy M, Clas, D., Vinik, A.I. (1992) Reversal of diabetes by the induction of islet cell neogenesis. Transplant. Proc. **24**,1027-1028

10 Bernard, C., Berthault, M.F., Saulnier, C., Ktorza, A. (1999) Neogenesis vs. apoptosis as main components of pancreatic beta cell ass changes in glucose-infused normal and mildly diabetic adult rats. FASEB J. **13**,1195-1205

11 Sharma A, Zangen DH, Reitz P, Taneja, M., Lissauer, M.E., Miller, C.P., Weir, G.C., Habener, J.F., Bonner-Weir, S. (1999) The homeodomain protein IDX-1 increases after an early burst of proliferation during pancreatic regeneration. Diabetes **48**,507-513

12 Guz, Y., Nasir, I., Teitelman, G. (2001) Regeneration of pancreatic beta cells from intra-islet precursor cells in an experimental model of diabetes. Endocrinology **142**,4956-4968

13 Dor, Y., Brown, J., Martinez, O.I., Melton, D.A. (2004) Adult pancreatic beta-cells are formed by self-duplication rather than stem-cell differentiation. Nature **429**,41-46

14 Lechner, A., Leech, C.A., Abraham, E., Nolan, A.L., Habener, J.F. (2002) Nestin-positive progenitor cells derived from adult human pancreatic islets of Langerhans

contain side population (SP) cells defined by expression of the ABCG2 (BCRP1) ATP-binding cassette transporter. Biochem. Biophys. Res. Commun. **293**,670-674

15 Shook, D.,Keller, R. (2003) Mechanisms, mechanics and function of epithelial - mesenchymal transitions in early development. Mech. Dev. **120**:1341-1383

16 Phillips PA, McCarroll JA, Park S, Wu, M.J., Pirola, R., Korsten, M., Wilson, J.S., Apte, M.V. (2003) Rat pancreatic stellate cells secrete matrix metalloproteinases: implications for extracellular matrix turnover. Gut **52**,275–282

17 Omary, M.B., Lugea, A., Lowe, A.W., Pandol, S.J. (2007) The pancreatic stellate cell: a star on the rise in pancreatic diseases. J. Clin. Invest. **117**,50-59

18 Kordes, C., Sawitza, I., Müller-Marbach, A., Ale-Agha, N., Keitel, V., Klonowski-Stumpe, H., Häussinger, D. (2006) CD133+ hepatic stellate cells are progenitor cells. Biochem. Biophys. Res. Commun. **352**,410-417

19 Garcia-Escarp, M., Martínez-Muñoz, V., Sales-Pardo, I., Barquinero, J,, Domingo, J.C., Marin, P., Petriz, J. (2004) Flow cytometry-based approach to ABCG2 function suggests that the transporter differentially handles the influx and efflux of drugs. Cytometry **62**,129-138

20 Catalano, R.A., Lillie, R.D. (1975) Elimination of precipitates in oil red O fat stain by adding dextrin. Stain Technol. **50**,297-299

21 Kawazu, S., Kanazawa, Y., Hayashi, M., Ikeuchi, M., Nakai, T., Kosaka, K. (1980) Monolayer culture of human fetal and adult pancreas. Static and dynamic studies of insulin release in vitro. Horm. Metab. Res.**12**,354-360

22 Spurr, A.R. (1969) A low viscosity epoxy resin embedding medium for electron microscopy. J. Ultrastruc. Res. **26**,36-43

23 Reynolds ES. (1963) The use of lead citrate at high pH as an electron opaque stain in electron microscopy. J. Cell. Biol. **17**,208-212

24 Royer, P.J., Tanguy-Royer, S., Ebstein, F., Sapede, C., Simon, T., Barbieux, I., Oger, R.,Gregoire, M. (2006) Culture medium and protein supplementation in the generation and maturation of dendritic cells. Scand. J. Immunol. **63**:401-9.

25 Haixia, Huang., Xueming, Tang. (2003) Phenotypic Determination and Characterization of Nestin-Positive Precursors Derived from Human Fetal Pancreas. Laboratory Investigation **83**,539-547

26 Schwitzgebel, V.M., Scheel, D.W., Conners, J.R. Kalamaras, J., lee, J.E., Anderson, D.J., Sussel, L., Johnson, J.D., German, M.S.(2000) Expression of neurogenin3 reveals an islet cell precursor population in the pancreas. Development **127**,3533-3542

27 Shapiro, A.M., Lakey, JR., Paty, B.W., Senior, P.A., Bigam, D.L., Ryan, E.A. (2005) Strategic opportunities in clinical islet transplantation. Transplantation **79**,1304-1307

28 Gao, R., Ustinov, J., Pulkkinen, M.A., Pulkkinen, M.A., Lundin, K., Korsgren, O., Otonkoski, T. (2003) Characterization of endocrine progenitor cells and critical factors for their differentiation in human adult pancreatic cell culture. Diabetes **52**,2007-2015

29 Seeberger, K.L., Dufour, J.M., Shapiro, S.M., Lakey, J.R., Rajotte, R.V., Korbutt, G.S. (2006) Expansion of mesenchymal stem cells from human pancreatic ductal epithelium. Lab. Invest. **86**,141-153

30 Weissman, I.L., Anderson, D.J., Gage, F. (2001) Stem and progenitor cells: origins, phenotypes, lineage commitments, and trans-differentiations. Annu. Rev. Cell. Dev. Biol. **17**,387–403

31 Scharfmann, R. (2000) Control of early development of the pancreas in rodents and humans: implications of signals from the mesenchyme. Diabetologia **43**,1083-1092

32 Beattie, G.M., Levine, F., Mally, M.I., Otonkoski, T., O'Brien, J.S., Salomon, D.R., Hayek, A. (1994) Acid beta-galactosidase: a developmentally regulated marker of endocrine cell precursors in the human fetal pancreas. J. Clin. Endocrinol. Metab. **78**,1232-1240

33 Kim, S.K., Hebrok, M., Melton, D.A. (1997) Notochord to endoderm signalling is required for pancreas development. Development **124**,4243–4252

34 Yashpal, N.K., Li, J., Wang, R. (2004) Characterization of c-Kit and nestin expression during islet cell development in the prenatal and postnatal rat pancreas. Dev. Dyn. **229:**813-25

35 Fetsch, P.A., Abati, A., Litman, T., Morisaki, K., Honjo, Y., Mittal,K., bates, S.E. (2006) Localization of the ABCG2 mitoxantrone resistance-associated protein in normal tissues. Cancer Lett. **235**, 84-92

36 Tanaka, Y., Slitt, A.L.,Leazeer, T.M., Maher, J.M., Klaassen, C.D. (2005) Tissue distribution and hormonal regulation of the breast cancer resistence protein (Bcrp/Abcg2) in rats and mice. Biocehm.Biophys.Res.Commun. **326**, 181-187

37 Leslie, E. M., Deeley, R.G., Cole, S. P. Multidrug resistance proteins: role of P-glycoprotein, MRP1, MRP2, and BCRP (ABCG2) in tissue defense (2005) Toxicol. Appl. Pharmacol. **204**, 216-237

38 Apte MV, Haber PS, Applegate TL, Norton, I.D., McCaughan, G.W., Korsten, M.A., Pirola, R.C., Wilson, J.S. (1998) Periacinar stellate shaped cells in rat pancreas: identification, isolation and culture. Gut **43**,128-133

39 Kruse, M.L., Hildebrand, P.B., Timke, C., Fölsch, U.R., Scmidt, W.E. (2000) Isolation, long-term culture, and characterization of rat pancreatic fibroblastoid/stellate cells. Pancreas **23**,49-54

40 Esni, F., Taljedal, I.B., Perkl, A.K., Cremer, H., Christofori, G., Semb,H.(1999) Neural cell adhesion molecule (N-CAM) is required for cell type segregation and normal ultrastructure in pancreatic islets. J. Cell. Biol. **144**,325-337

41 Royer, P.J., Tanguy-Royer, S., Ebstein, F., Sapede, C., Simon, T., Barbieux, I., Oger, R., Gregoire, M. (2006) Culture medium and protein supplementation in the generation and maturation of dendritic cells. Scandinavian Journal of Immunology **63**,401-409

42 Ratineau, C., Duluc, I., Pourreyron, C., Kedinger, M., Freund, J.N., Roche, C. (2003) Endoderm- and mesenchyme-dependent commitment of the differentiated epithelial cell types in the developing intestine of rat. Differentiation **71**,163-169

43 Sttaford, D., White, R.J., Kinkel, M.D., Linville, A., Schilling, T.F., Prince, V.E. (2006) Retinoids signal directly to zebrafish endoderm to specify insulin-expressing beta-cells. Development **133**,949-956

44 Yue, F., Cui, L., Johkura, K., Ogiwara, N., Sasaki, K. (2006) Glucagon-like peptide-1 differentiation of primate embryonic stem cells into insulin-producing cells.Tissue Engineering **12**,2105-2115

45 Abraham, E.J., Leech, C.A., Lin, J.C., Zulewski, H., Haberner, J.F. (2002) Insulinotropic hormone glucagons-like peptide-1 differentiation of human pancreatic islet-derived progenitor cells into insulin-producing cells. Endocrinology **143**,3152-3161

46 Hui, H., Wright, C., Perfetti, R. (2001) Glucagon-like peptide 1 induces differentiation of islets duodenal homeobox-1-positive pancreatic ductal cells into insulin-secreting cells. Diabetes **50**,785 –796

FIGURE LEGENDS

Fig. 1. Mitoxantrone induced apoptosis in digested fresh pancreata as measured by Hoechst 33342 staining.
Results are shown as apoptotic cells as a percentage of total number of cells and expressed as mean ± S.E.M. values of the data obtained from four independent experiments performed in 4–5 wells. * p<0,001 $^{\#\#}p < 0.01$

Fig. 2 ABCG2 expression, and drug uptake and retention assays in primary cell cultures (mitoxantrone-resistant cells and unselected cells)
(A) One-hour drug accumulation assay with and without verapamil. The cells were preincubated with 5µM verapamil for 15 min. Subsequently, cells were treated with 8 µM mitoxantrone and assayed for drug accumulation as described in "Materials and Methods." Each condition is the mean of three experiments ± SD. Verapamil increased the intracellular concentration of mitoxantrone in the mitoxantrone-selected drug-resistant cells. The experiment was performed in triplicate, and a representative histogram was shown
(B) The ABCG2 expression in the cells from cultures: unselected cells (line 1) and mitoxantrone-resistant cells at Stage 2 (line 2) was determined by RT-PCR. The ARIP cell line was used as a positive control of the reaction (Control), –RT corresponds to amplification in which reverse transcriptase was excluded from the reaction (negative control).

Fig. 3 Establishment and Characterization of a Cell Line from mitoxantrone-resistant cell population.
(A) Nestin, Thy1.1 and N-CAM protein expression was detected by immunostaining in culture from mitoxantrone-selected drug-resistant cells. Autofluorescence was also observed. Hovewer, no expression was observed in cultures from unselected cells, used as a control. The unselected cells were incubated in 1µg/mL DAPI solution for 30 min in the dark. (X20 original magnification). (B) The mitoxantrone-resistant cells became overgrown by cells with a fibroblastoid morphology (a,b). Spontaneously, some cells began to form three-dimensional cell clusters (c,d,e). (C) The immunophenotyping results were confirmed by RT-PCR from one µg of total RNA of the cells unselected cells (line 1) and mitoxantrone-resistant cells at Stage 2 (line 2) and mitoxantrone-resistant cells at Stage 3 (line3). The ARIP cell line was used as a control of the reaction (line 4). The primers were designed across intron(s), when possible, and their sequences and product sizes are listed in the Table 2. The thermal cycle was repeated 38 times in all the genes analysed.

Fig. 4 Mitoxantrone-resistant cells were phenotyped by immunofluorescence and RT-PCR using pancreatic stellate markers.
(A) Mitoxantrone-resistant cells at Stage 2 express the markers: alfa-Actin, GFAP, vimentin, desmin, and chromogranin A. To confirm the presence of the vitamin A stored in the fat droplets, oil red staining was performed. (B) Disaggregated from mitoxantrone-resistant cells at stage 3 were immunophenotyped for the same markers, including the oil red staining. Negative controls (Neg) were used. (X20 original magnification). (C) These results were confirmed by RT-PCR using one µg of total RNA of the mitoxantrone-resistant cells in both stages (stage 2 and stage 3). Control cell lines were used as a control reaction.

Fig. 5 Pancreatic gene expression profiles
(A) RT-PCR analysis of the gene expression profiles was preformed using one µg of total RNA of unselected cells and mitoxantrone-resistant cells. Genes from pancreatic lineage were identified and compared their expression using different media: basal medium (M 0), Medium 1 (M1) and Medium 3 (M 3). Different cell lines were used as a control of the RT-PCR reactions. All primers were designed across intron(s), when possible and their sequences and product sizes are listed in the Table 2. The thermal cycle was repeated 38 times in the gene analysis.
(B) Effect of adenovirus-mediated extopic expression of ngn3 on key developmental transcription factors and pacneratic marker expression in mitoxantrone-resistant cells at stage 3. Gene profiling expression of: Neuro D, Pax 6, Pax 4, Pdx-1, Nestin, ABCG2, Insulin, Glucagon, IAPP, PC1/3, PC2, CK19, Thy1.1 and N-CAM mRNA were assayed by RT-PCR in mitoxantrone-resistant cells at stage 3 after infection with adenovirus expressiong Ngn3 (AdCMV-ngn3) or as a control of efficiency of infection with a adenovirus expressing β-galactosidase (AdCMV-β-gal). mRNA was harvested from mitoxantrone-resistant cells at stage 3 24 hours after infection with an adenovirus expressing Ngn3 (AdCMV-ngn3) or as a control adenovirus expressing β-galactosidase (AdCMV-β-gal). The numbers of PCR cycles were 25 for TBP, 30 for Ngn3, and 38 for the other transcripts. (C) Gene expressions of Pdx-1 and GLP1 receptor were detected by RT-PCR and quantifed their expression by RT-PCR Real-Time in mitoxantrone-resistant cell cultures with basal medium (M0), Medium 1 (M1) and Medium 2 (M 2). The Pdx-1 values from cell cultures with M 0 were taken as reference and values were normalised to housekeeping TBP mRNA levels. The bars indicate the SEM of three independent experiments performed in duplicate and * Indicate statistical significance with $p<0.05$.

Fig.6 The photomicrographs showed a representative images of co-immunolocalization of different markers by cytospin-prepared cells obtained from disagregated cellular clusters after treatment with medium 3. The markers were visualized in red: c-peptide, green: insulin, vimentin, CK19, GFAP, alfa-actin, and yellow as the merges. The MIN-6 cells were used for the immunohistochemistry control. (X40 original magnification (a-l), X20 original magnifications (m-r).

Fig. 7 Ultrastructural changes and insulin release in the Mitoxantrone-resistant cells at stage 3 after differentiation treatment with medium 3.
(A) Transmission electron micrographs of undifferentiated cells (a-d) show high hypertrophy in the rough endoplasmic reticulum (rER), lipid droplets (LD), lysosomes (L) and collagenous fibers (CF). Two types of electron-dense chromatin structure were observed (Ch). However, the differentiated cells (e-h) presented a homogenous size with a round nucleus (N), at times indented, abundant mitochondria (M), and electron-dense granules in the cytoplasm were observed (g). (B) Insulin secretion after 1 hour of glucose stimulation at 20 mM *vs*. 2.8 mM. The results were normalized to 100 cell clusters (n=3) * $p< 0.05$ (employing Student's t-test).

Table 1 Antibodies for the characterization of the cell culture

Anti-rat or human	Dilution	Fluorochrome	Source
Nestin	1/100	Cy™2	556309 BD Biosciences Pharmingen, Mississauga, CA, USA
Thy-1.1 (CD90)	1/100	fluoresceine	554897 BD Biosciences Pharmingen, Mississauga, CA, USA
N-CAM	1/100	Cy™2	L0015, USBiological, Massachusetts, USA
GFAP	1/500	Cy™2	Chemicon International
Alfa-Actin	1/10	Cy™2	A0760-22 USBiological, Massachusetts, USA
Vimentin	1/100	Cy™2	MAB3400 Chemicon International
Chromogranin A	1/100	Cy™3	RB-9003-PO Bionova, Westinghouse, CA, USA
Desmin	1/100	Cy™2	MCA849 Serotec, Oxford, UK
C-peptide	1/100	Cy™3	4023-01 Linco Research, Missouri, USA
Cytokeratin-19	1/1000	Cy™2	Z-0622 Dako, Carpinteria, CA, USA
Insulin	1/2000	AMCA	A0564, Dako, Carpinteria, CA, USA

Anti-rabbit Cy™2 Jackson Immuno Research 711-225-152, anti-guinea pig-AMCA Jackson Immuno Research 706-155-148 and anti-mouse Cy™3 Jackson Immuno Research 705-225-147

Table 2. Primers for reverse transcription-polymerase chain reaction

Gene	Primers	Amplicon	T	Accession No.
ABCG2	Forward: ACAAAAGCTGAATTAGATCAACTT Reverse: GAGATTCACCAAGAGGCCAG	641	59	NM_181381
Nestin	Forward: GCGGGGCGGTGCGTGACTAC Reverse: GCAAGGGGGAAGAGAAGGATGT	523	62	NM_012987
Thy1.1	Forward: CGCTTTATCAAGGTCCTTACT Reverse: GCGTTTTGAGATATTTGAAGGT	343	52	P01830
NCAM	Forward: CAGCGTTGGAGAGTCCAAAT Reverse: TTAAACTCCTGTGGGGTTGG	300	54	NM_031521
Vimentin	Forward: GCCAGCAGTATGAAAGTGTG Reverse: AGTGGGTGTCAACCAGAGGAA	496	60	NM_031140
Desmin	Forward: AGACTTGACTCAGGCAGCCAAT Reverse: CGGAAGTTGAGAGCAGAGAAGG	384	60	NM_022531
GFAP	Forward: TGGCCACCAGTAACATGCA Reverse: GACTCCTTAATGACCTCGCCAT	538	60	NM_017009
Alfa-Actin	Forward: ATCCGATAGAACACGGCATC Reverse: AGAAGAGGAAGCAGCAGTGG	500	60	RGD:1559154
Chromogranin A	Forward: CGGCTTTGGCGCTTCTGCT Reverse: CTTGGAGGGGGCTTCTGATGCT	401	60	NM_021655
Pdx-1 Real-Time	Forward: CCGCGTTCATCTCCCTTTC Reverse: CTCCTGCCCACTGGCTTTT			NM_022852
Pdx-1	Forward: GAGCCCAGCCGCGTTCATCT Reverse: CCCCGCTCGTTGTCCCGCTACTA	318	60	NM_022852
NGN3	Forward: TGGCGCCTCATCCCTTGGATG Reverse: CAGTCACCTGCTTCTGCTTCG	160	60	MN_021700.1
Glucagon	Forward: ATCATTCCCAGCTTCCCAGA Reverse: CGGTTCCTCTTGGTGTTCAT	161	57	NM_012707
IAPP	Forward: AGTCCTCCCACCAACCAATGT Reverse: AGCACAGGCACGTTGTTGTAC	220	62	NM_012586
Insulin	Forward: TGGCCCTGTGGATCCG Reverse: AGTTGCAGTAGTTCTCCAGCTGG	329	52	NM_019129
GLUT2	Forward: GACACCCCACTCATAGTCACAC Reverse: CAGCAATGATGAGAGCATGTG	270	57	P12336
TBP Real- Time	Forward: TTCGTGCCAGAAATGCTGAA Reverse: TTCGTGCCAGAAATGCTGAA			NM_001004198
TBP	Forward: ACCCTTCACCAATGACTCCTATG Reverse: ATGATGACTGCAGCAAATCGC	190	60	NM_01004198

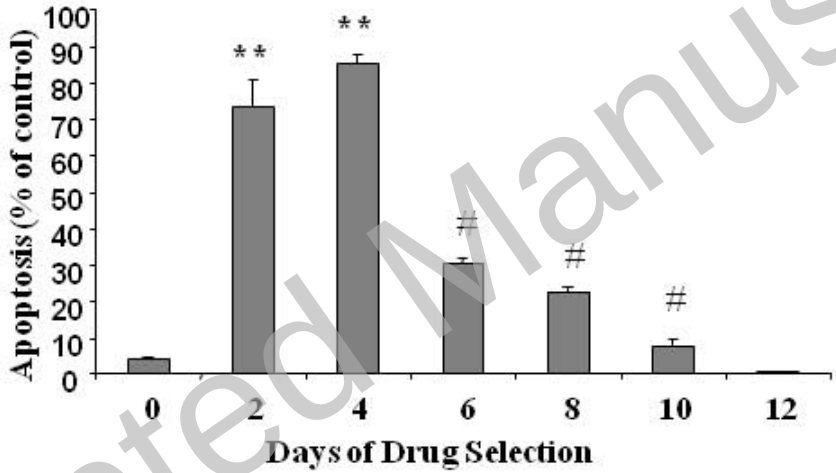

Fig.1
E.Mato et al.

Biochemical Journal Immediate Publication. Published on 20 Apr 2009 as manuscript BJ20081466

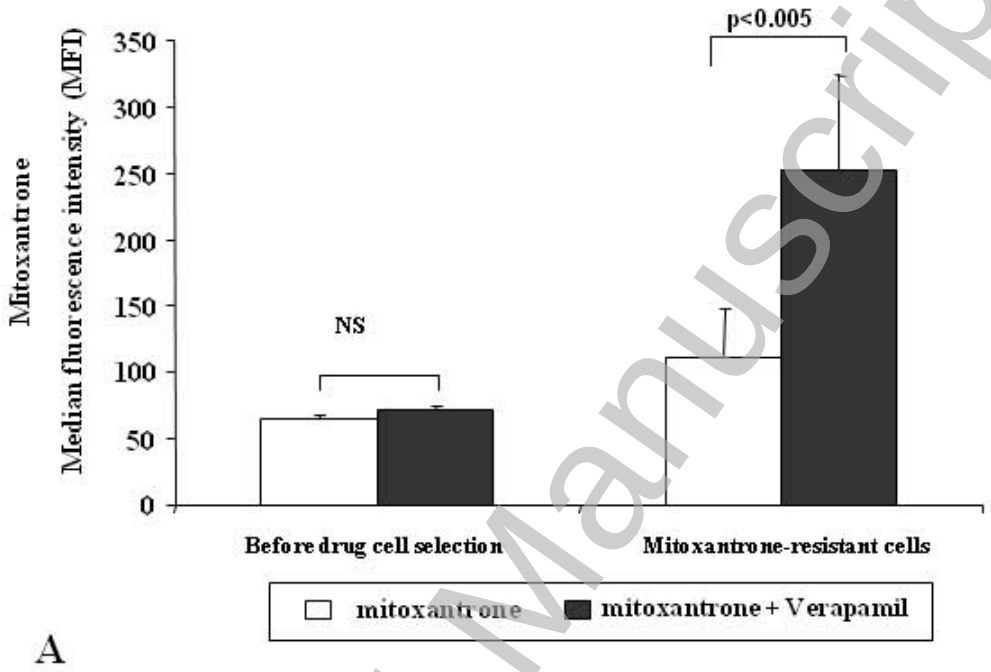

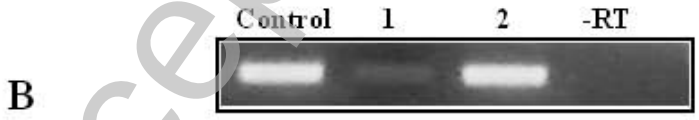

Fig. 2
E.Mato et al.

Biochemical Journal Immediate Publication. Published on 20 Apr 2009 as manuscript BJ20081466

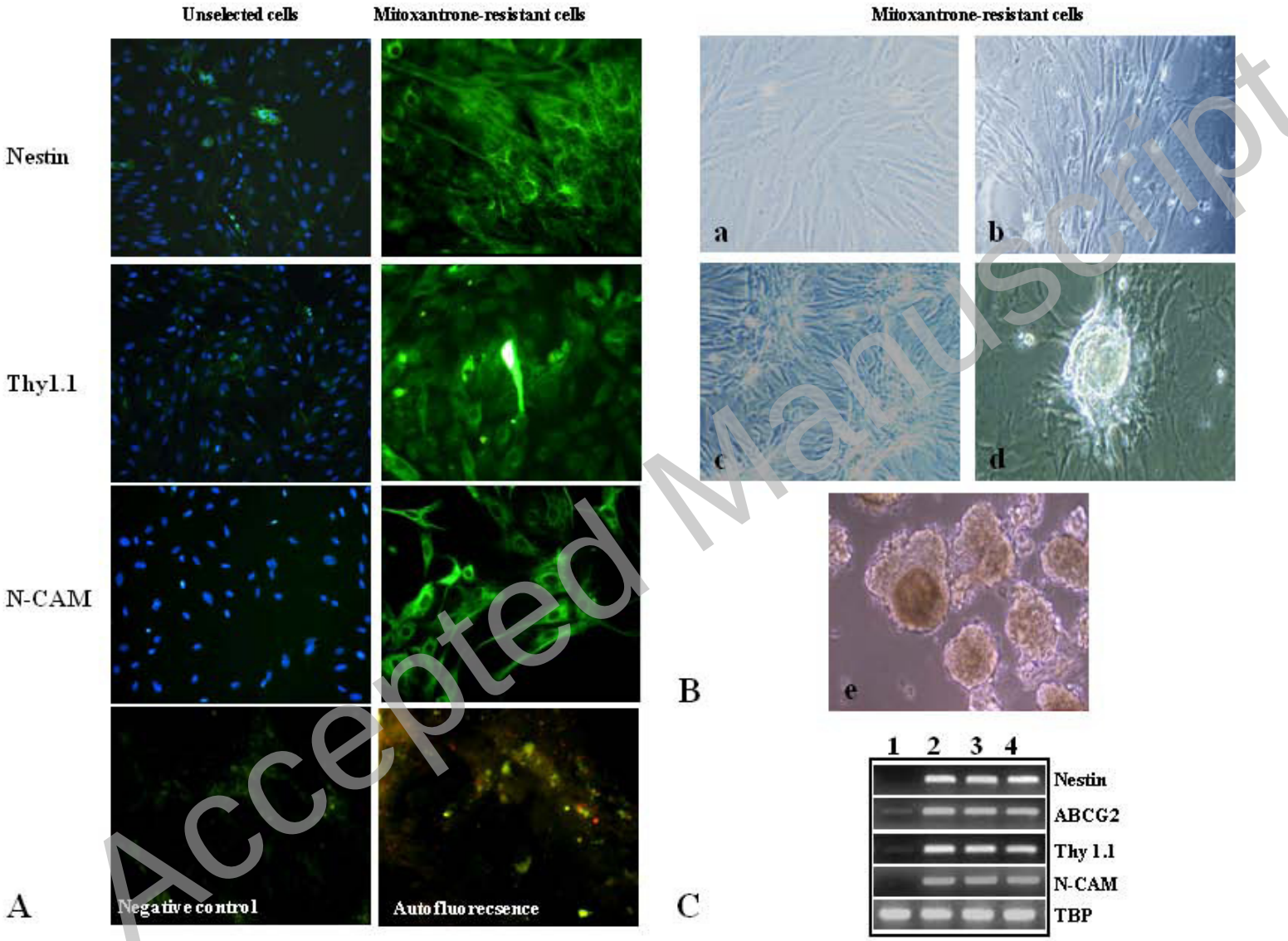

Fig.3
E.Mato et al.

Biochemical Journal Immediate Publication. Published on 20 Apr 2009 as manuscript BJ20081466

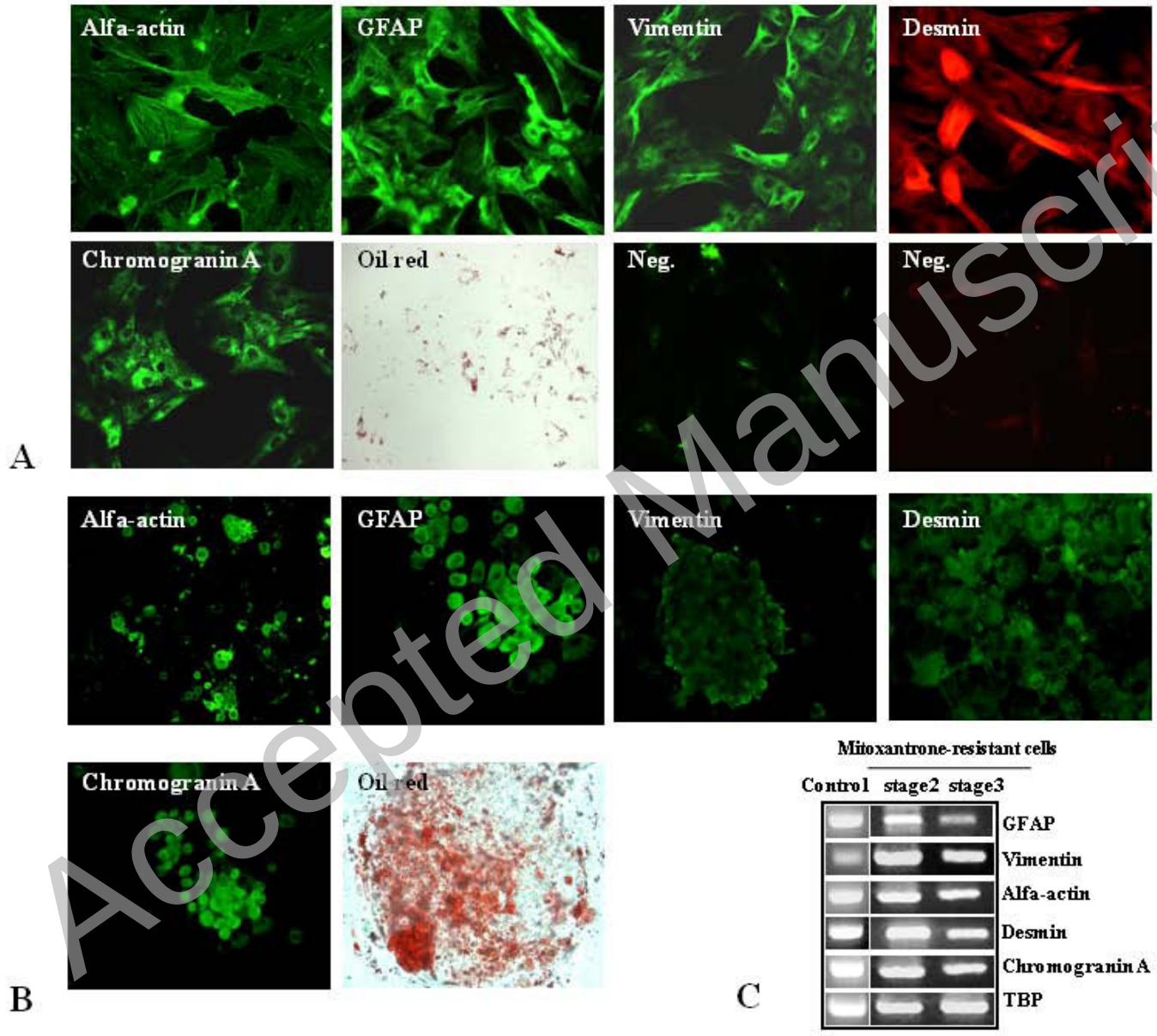

Fig.4
E.Mato et al.

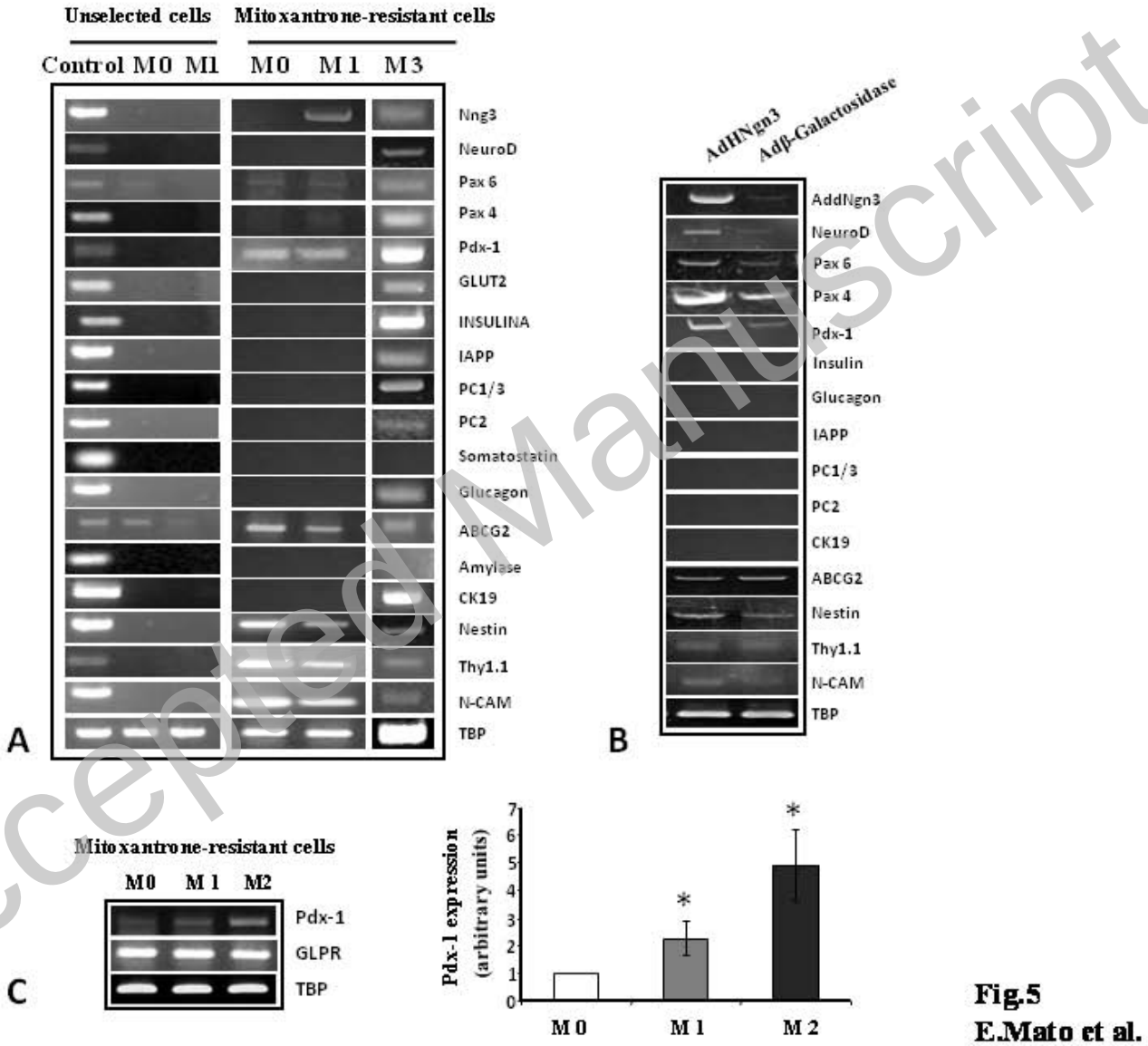

Fig.5
E.Mato et al.

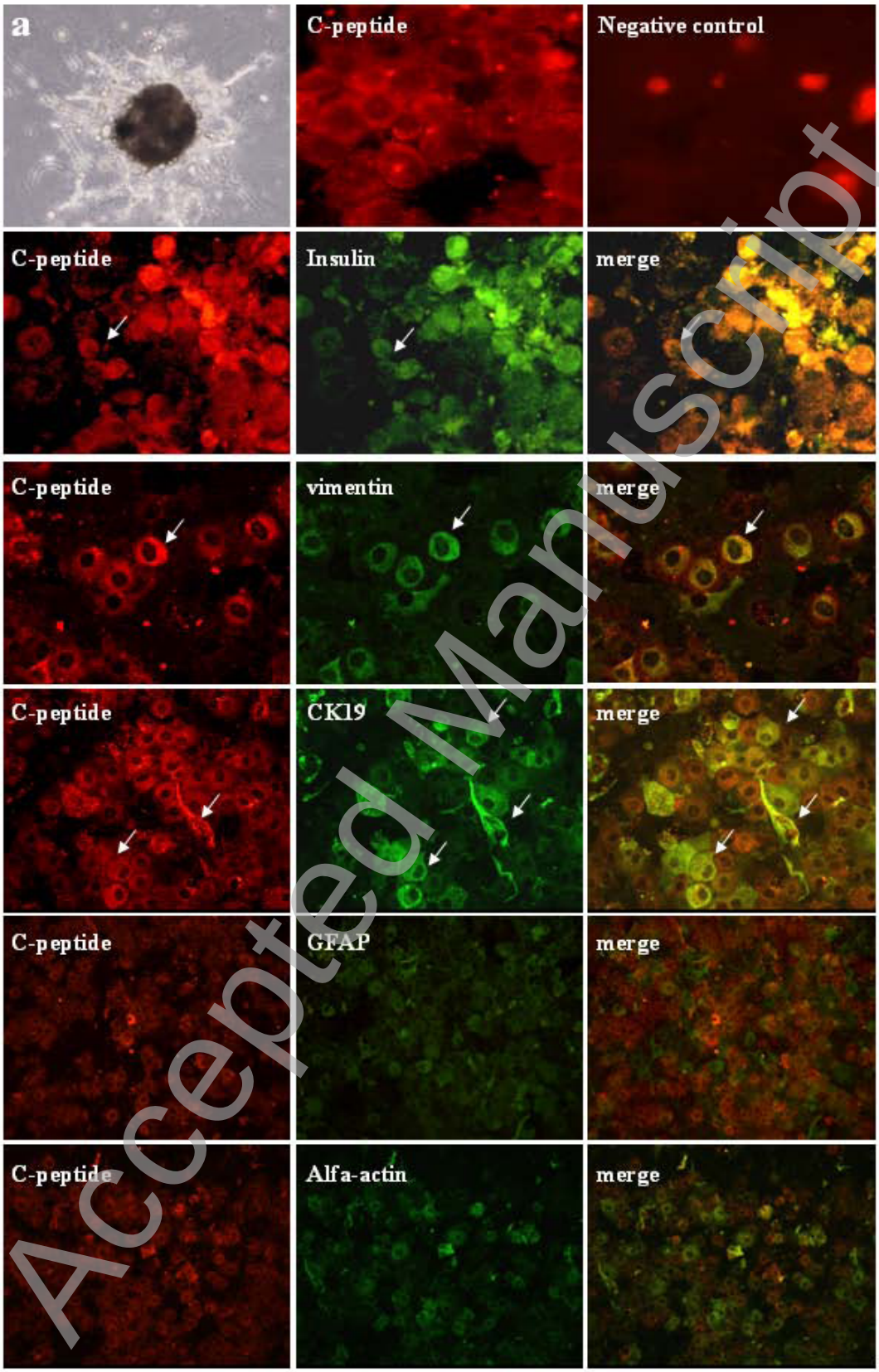

Fig.6
E.Mato et al.

Biochemical Journal Immediate Publication. Published on 20 Apr 2009 as manuscript BJ20081466